Challenge Journal of Concrete Research Letters

Research Article

Predictability of concrete damage level by non-destructive test methods

Boğaçhan Akça [a,*], Süleyman Bahadır Keskin [a], Aysu Göçügenci [a]

[a] *Department of Civil Engineering, Muğla Sıtkı Koçman University, 48000 Muğla, Turkey*

ABSTRACT

Non-destructive methods have many advantages over traditional test methods, especially since it does not damage the specimen, it can be used multiple times on the same specimen. These advantages also provide a great benefit in terms of following the property development in concrete as the same specimens are used which eliminates the variations related to the specimens. In this study, it is aimed to determine the damage amount of concrete produced with different binders by electrical bulk resistivity, resonance frequency, and ultrasonic pulse velocity methods. Firstly, concretes containing different binders were produced, and along with the mechanical properties, ultrasonic wave velocity, resonance frequency, and electrical resistivity values of the produced concrete were determined at the 7, 28, and 90 days. Besides, the specimens were subjected to gradually increased compressive loads and non-destructive methods were used to estimate the extent of damage on specimens. It was attempted to establish a relationship between the damage on concrete specimens and the results obtained by non-destructive methods. Consequently, the compressive strength, electrical resistivity, ultrasonic pulse velocity and resonance frequency values of all specimens increased with the advancing age. It was concluded that the resonant frequency method is more successful than other methods in estimating the amount of damage in concrete.

ARTICLE INFO

Article history:
Received 23 August 2021
Revised 2 October 2021
Accepted 1 November 2021

Keywords:
Non-destructive testing
Concrete
Damage
Mineral admixtures
Compressive strength

1. Introduction

Considering the wide use of concrete as a construction material, degradation of concrete structures is also a great concern. The extent of concrete damage can be evaluated in many ways. Although taking cores from the existing structures is a common method, in recent years, non-destructive testing methods have been used frequently. As concrete is mainly resistant to compressive forces, the compressive strength and some physical properties of concrete can be estimated by non-destructive testing methods. Non-destructive testing methods can be used to determine the concrete quality in new constructions, as well as to determine the properties of the existing structures (ACI 228.2R-98, 1998). By using non-destructive testing methods, an idea about the parameters such as the absorption capacity of concrete, modulus of elasticity, compressive strength, moisture content, and electrical resistance of concrete can be obtained (Breysse, 2012).

One of the novel non-destructive techniques on concrete uses bulk electrical resistivity to evaluate the concrete's durability. The electrical resistivity of concrete depends on the concrete's water/cement ratio, mineral and chemical admixtures, age, aggregate type, degree of saturation, and the environmental conditions in which it is cured (Layssi et al., 2015). Since the alternating current is employed in the electrical resistivity test, in order to determine the resistivity, impedance and the phase angle values are collected and transformed to resistance and resistivity afterwards (Layssi et al., 2015). In a study of electrical resistance, concrete mixtures were prepared with 4 different types of cement with varying water/binder ratios while, the amount of cement and aggregate type

* *Corresponding author*. E-mail address: bogachanakca26@gmail.com (B. Akça)
ISSN: 2548-0928 / DOI: https://doi.org/10.20528/cjcrl.2021.04.004

were kept constant (Medeiros-Junior et al., 2016). According to this research, it is shown that the electrical resistance of concrete can also be affected by the type of cement (Medeiros-Junior et al., 2016). Besides, parameters that can be obtained from the rapid chloride ion penetration test were shown to be obtained by the electrical resistivity test (Shane et al., 1999). Bearing in mind that the rapid chloride ion penetration test takes quite a long time, the electrical resistance test is more advantageous from the practicality point of view. Moreover, some studies showed that the increase in the compressive strength of concrete causes an increase in the electrical resistivity of concrete (Lübeck et al., 2012; Helal et al., 2015). This is because as the compressive strength of the concrete increases, hydration products fill the voids inside the concrete. In damaged concrete, due to the increase in the size of the voids and the number of voids in the damaged parts of concrete, some changes may occur in the electrical resistivity. In this research, the relationship between the damage amount of concrete prepared with different mineral admixtures and electrical resistivity was tried to be found.

Ultrasonic pulse velocity is a common method to evaluate the concrete properties non-destructively. The quality, homogeneity, void state, crack state and crack depth of the concrete can be determined by using an ultrasonic pulse velocity test (ASTM C597-97, 1997). Ultrasonic pulse velocity can be affected by w/c ratio, the maximum size of coarse aggregates, and cement type (ASTM C597-97, 1997; Trtnik et al., 2009). Properties and types of aggregates can affect the compressive strength as well as the ultrasonic pulse velocity of the concrete specimens (Trtnik et al., 2009).

Qasrawi (2000) researched that concrete strength can be predicted by using NDT methods such as ultrasonic pulse velocity and rebound hammer. Also, Mohammed and Mahmood (2016) conducted a study on how aggregate size affects ultrasonic pulse velocity. In their study, brick fractions were used as coarse aggregate in different sizes, and it was concluded that the ultrasonic pulse velocity increased as the aggregate size increased in concrete.

Ultrasonic pulse velocity alongside with compressive strength is affected by the age and curing period of the concrete specimens as well. Demirboğa et al. (2004) investigated ultrasonic pulse velocity and compressive strength parameters in high-volume mineral admixture concrete. In their study, it was observed that both compressive strength and ultrasonic pulse velocity results increased with advancing age and curing period.

Another non-destructive technique adopted in this study is resonance frequency testing. There are two ways to determine the resonance frequency of the concrete: the forced resonance method and the impact resonance method. In the impact resonance method which is used in this experimental work, the specimen is struck with the impactor, and the specimen response is measured with the accelerometer.

Dynamic modulus of elasticity can be estimated by using the resonance frequency test method (ASTM C215-08, 2008). But the result can be affected by the manufacturing process, mix design, aggregate properties, specimen size, and curing conditions of the concrete (ASTM C215-08, 2008; Helal et al., 2015). One study shows that the self-healing capability of the concrete specimens which are prepared by different pozzolanic materials such as ground granulated blast furnace slag and Class F fly ash can be determined by using NDT methods such as electrical impedance, rapid chloride permeability test, and resonance frequency (Yildirim et al., 2015).

In the literature, many studies are explaining the relationship between non-destructive testing methods and the properties of concrete (Kolluru et al., 2000). In some of these studies, concrete specimens are prepared with different cementitious materials, and some specimens are stored and cured at different temperatures (Hong et al., 2021). For several studies, even the damage of concrete was individually investigated with various NDT methods (Chun et al., 2020). However, there is no study that seeks to demonstrate the relationship between the damage of the concrete specimens and non-destructive testing methods for concretes with different binders as far as the authors' concern.

In this study, three NDT methods: electrical resistivity, ultrasonic pulse velocity, and resonance frequency were used. Concrete specimens which were prepared with different pozzolans such as fly ash, silica fume, and ground granulated blast furnace slag, were damaged to various levels of their compressive strength value. The extent of the damage was expressed as a percentage of compressive strength of the specimens, ranging from 0% to 100% in increments of 25%. At the end of this study, the relationship between NDT results and damage level of concrete specimens was established.

2. Experimental Program

2.1. Materials and mix design

In this study, the main goal is to find a relation between the degree of damage on a concrete specimen and the results of electrical resistivity, ultrasonic pulse velocity, and resonant frequency tests. For this purpose firstly, the concrete mixtures were designed and specimens were prepared according to ACI 211.1-91 guideline and ASTM C192 standard, respectively (ACI 211.1-91, 2002; ASTM C192 / C192M-14, 2014).

For concrete mix design, a target compressive strength of 25 MPa is specified for the mixture without any cement replacement materials which serves as a control mixture. For the remaining three mixtures some of the Portland cement was replaced with fly ash, silica fume and ground granulated blast furnace slag. The replacement level was based on conventional usage of these binders.

CEM I 42.5 R type ordinary Portland cement (OPC) was a product of Oyak Cement Factory, fly ash (FA) was obtained from Yatağan Thermal Power Plant, silica fume (SF) from Eti Metallurgy Inc. in Antalya, and finally the ground granulated blast furnace slag (GGBFS) from Iskenderun Iron and Steel Plant. The chemical compositions and physical properties of the binding materials are provided in Table 1.

As mentioned previously, 25 MPa compressive strength was targeted in the control mixture. In the mixtures containing FA, SF, and GGBFS produced to investigate the effects of different binder materials, the replacement levels of 20, 5, and 20% were used, respectively. The proportions of the ingredients of produced concretes are presented in Table 2.

2.2. Specimen preparation

For all the compressive strength and NDT tests conducted throughout the experimental research, cylindrical specimens with 10 cm diameter and 20 cm height were used. During the preparation of the fresh concrete, firstly aggregates and half of the mixing water were introduced to a drum-type concrete mixer. The mixer was operated until the entire surface of the aggregates was wetted. After then, Portland cement, mineral admixtures (if used), and all the remaining mixing water were introduced into the mixer. The mixer was restarted again, and the mixing process was completed when a homogeneous mixture was obtained. Once the fresh concrete was prepared, cylindrical molds with a diameter of 10 cm and a height of 20 cm were filled with fresh concrete in two layers and compacted as seen in Fig. 1.

Table 1. Chemical composition and physical properties of binding materials.

	PC	FA	GGBFS	SF
SiO_2 (%)	18.69	50.04	38.4	91.96
CaO (%)	61.87	11.21	34.48	0.62
Al_2O_3 (%)	4.74	22.85	10.96	1.20
Fe_2O_3 (%)	3.37	8.02	0.81	0.84
MgO (%)	3.36	2.23	7.14	1.02
SO_3 (%)	2.93	0.78	1.48	0.12
K_2O (%)	0.63	2.50	0.86	1.16
Na_2O (%)	0.19	2.27	0.18	0.67
Specific Gravity	3.15	2.28	2.79	2.20
Blaine Fineness (m^2/kg)	342	285	425	-

Table 2. Concrete mix proportions.

	PC (kg/m^3)	FA (kg/m^3)	SF (kg/m^3)	GGBFS (kg/m^3)	Coarse aggregate (kg/m^3)	Fine aggregate (kg/m^3)	Water (kg/m^3)
PC-Mix	400	0	0	0	960	714	216
FA-Mix	320	80	0	0	960	619	216
SF-Mix	380	0	20	0	960	621	216
GGBFS-Mix	320	0	0	80	960	636	216

Fig. 1. Cylindrical concrete specimens.

After this process, molds were left for 24 hours under laboratory conditions, then the specimens were removed from the molds and cured under water at 23°C till the age of testing for the development of strength. Afterward, in each mixture, 6 specimens were produced and used for the ages of 7, 28 and 90 days. 3 of the specimens were used as control specimens and the other 3 specimens were used as test specimens. The compressive strength of the specimens in the control group was determined under a constant loading rate of 0.3 MPa/s according to the ASTM C39 as seen in Fig. 2 (ASTM C39, 2021). For the control specimens, NDT measurements were taken from the sound specimens before testing, and also after loading the specimens to failure for each experimental method. For the test group, the specimens were loaded gradually to 0%, 25%, 50%, 75%, and 100% of their compressive strength, and NDT tests were performed prior to loading and also after each level of damage. The damage levels were calculated according to the compressive strength values of control specimens at failure.

The electrical resistivity test was carried out at a frequency of 1 kHz of alternating current. To provide the uninterrupted current flow, sponges that were wetted to a constant weight of 21 g were placed between the specimens and the electrode layers. Afterward, as seen in Fig. 3, cylindrical specimens were placed between two electrodes, and the measurements were taken. Then the measured resistance values were used to calculate the electrical resistivity of the specimens.

Fig. 2. Compression test.

Fig. 3. Electrical resistivity test.

The ultrasonic pulse velocity test was carried out at a frequency of 54 kHz. During this test, ultrasound gel was applied as a contact material between transducers and the specimen. The transmitting and receiving transducers were placed on the parallel surfaces of the concrete specimen and measurements were taken through direct transmission as seen in Fig. 4.

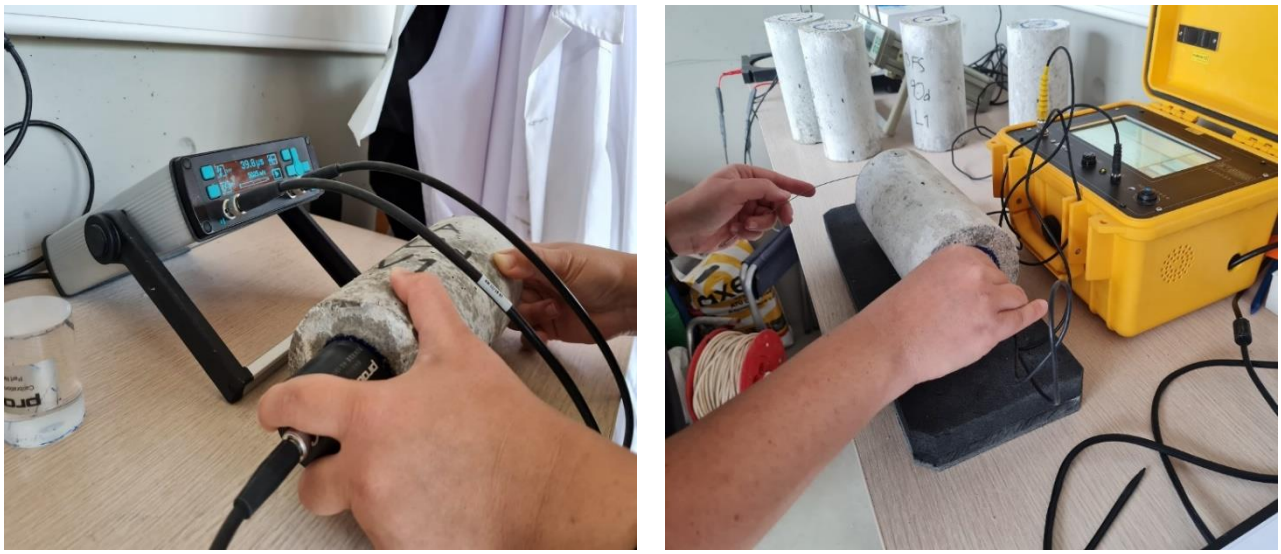

Fig. 4. Ultrasonic pulse velocity test and resonance frequency test.

The resonance frequency test was operated via a resonance frequency meter with maximum sampling frequency of 100 kHz. After the dimensions and mass of specimens are input into the frequency meter, the specimens are struck with a 19 mm diameter-steel ball impactor from one end regarding the longitudinal vibration mode. The specimen vibrations are obtained with the accelerometer from the other end of specimen and the obtained frequency values are measured with frequency meter as seen in Fig. 4.

3. Result and Discussion

3.1. Compressive strength

The compressive strength values in the graph were obtained as a result of compression test applied on control specimens of each mixture till their failure. Depending on the mineral admixtures used in the production of concrete mixtures, as seen in Fig. 5, the development of the compressive strength differs. The compressive strengths of concrete mixtures which were prepared by different mineral admixtures were lower than the control mixture at early ages and similar or higher at later ages. This situation is expected as they differ in activity and rate of reaction (Shi et al., 2009; Duan et al., 2013; Gonen and Yazicioglu, 2007; Hassan et al., 2000).

The control mixture showed the highest compressive strength only at 7 days due to the rapid hydration of Portland cement compared to other mineral admixtures. Although mixtures apart from the control mixture had similar compressive strengths at early ages, the use of SF resulted in slightly higher strength. This can be attributed to the lower replacement level of SF (5%) compared to FA and GGBFS. However, at the end of the 28th day, the difference became more pronounced in favor of the mixture containing silica fume as it gained a considerably higher strength than the other mixtures. Similar situations were confirmed by several authors in the literature (Ozturk et al., 2020; Gokce et al., 2019; Gupta et al., 2021). Although the compressive strength of concretes containing ground granulated blast furnace slag and fly ash was lower than the control mixtures as of this age, the GGBFS mixture reached a strength close to the control mixture with the effect of high CaO content. At 90 days, SF, and GGBFS mixtures reached higher compressive strength than the control mixture and FA reached a strength close to the control mixture as a result of pozzolanic activity and secondary hydration.

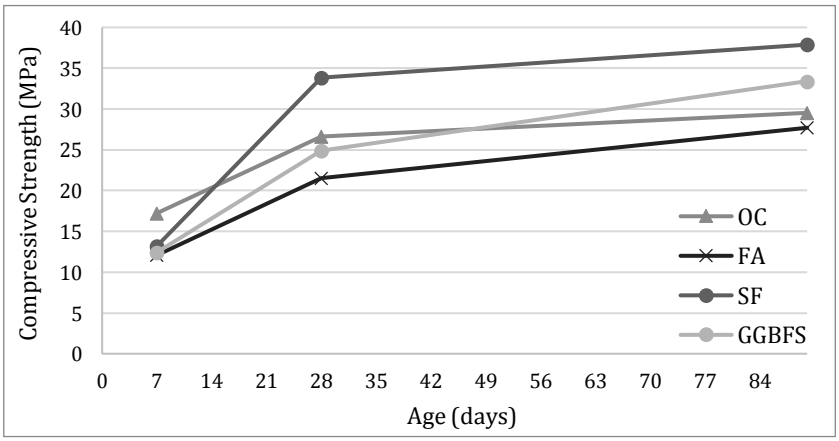

Fig. 5. Compressive strength development.

3.2. Electrical resistivity

For obtaining the electrical resistivity values, the impedance values at the lowermost phase angles were determined. Nevertheless, for the 1 kHz frequency at which the measurements were taken, the phase angles were always 0° hence, impedance values were equal to the resistance. Electrical resistivity could easily be calculated by multiplying the resistance with the cross-sectional area and dividing it by the length of the specimen. When the graph was observed, it should be mentioned that in each mixture, the first, second and third points provide the values for the ages of 7, 28 and 90 days respectively. To distinguish the results, 7 days values were presented with solid filled markers, 28 days values with blank markers and 90 days values with pattern filled markers. It was understood from the results obtained that the resistivity values increase with age. This situation can be explained by the decrease in the capillary voids as specimen age increases. Similarly, electrical resistivity values also increased in the same manner when the sound specimens were damaged due to the cracks formed as a result of loading. The reason for the increase in resistivity is due to the difficulty of electrical current to pass through the formed cracks and voids when the moisture content is kept constant. Studies showed that electrical resistivity increases with specimen age and compressive strength (Medeiros-Junior et al., 2016; Lübeck et al., 2012; Valcuende et al., 2020; Bem et al., 2018; Ferreira and Jalali, 2010; Duran-Herrera et al., 2019; Ghoddousi and Saabadi, 2017; Tumidajski, 2005; Gastaldini et al., 2009). As seen in Fig. 6, a similar trend is also observed in this study.

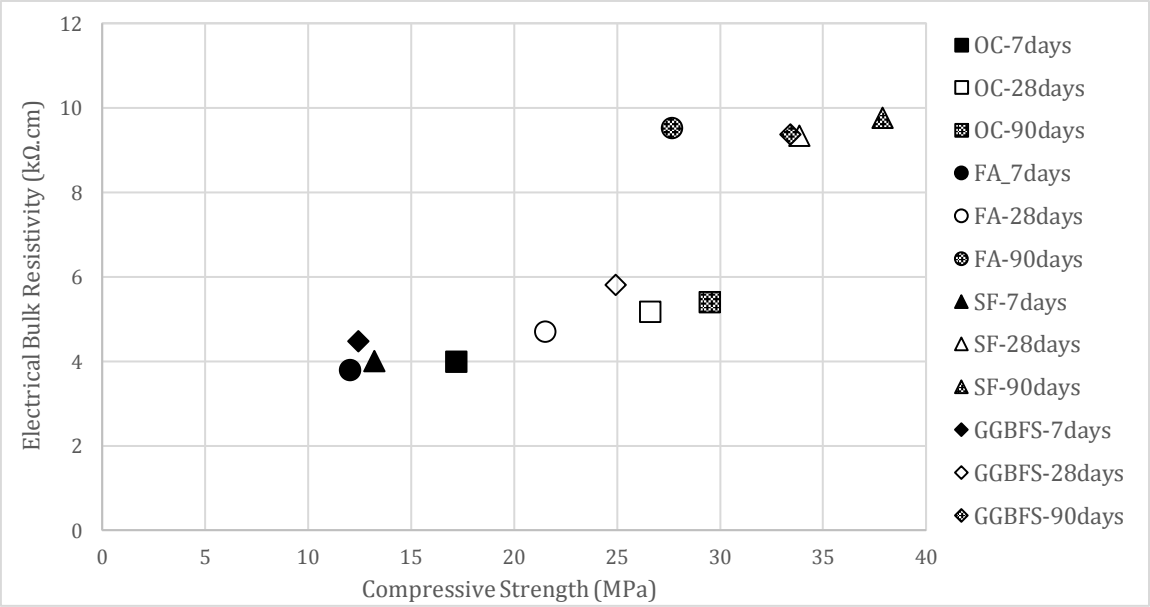

Fig. 6. Electrical bulk resistivity vs. compressive strength.

In addition, the measurement of the electrical resistivity of concrete is realized by the ion transfer through the water-filled pores in the concrete. Since the chemical compositions of the mineral admixtures used in this study are different from ordinary Portland cement as seen in Table 1, the electrical resistivity of the concrete specimens prepared by using them is also different as they alter the chemistry of the pore solution (Duran-Herrera et al., 2019; Gastaldini et al., 2009; Shi, 2004). The electrical resistivities of the control specimens of each mixture for the ages of 7, 28 and 90 days before (undamaged state) and after (failed state) the application of compressive loads up to the failure of the specimens are shown in Fig. 7. Also, the response of electrical resistivity to gradually increased damage levels are shown in Fig. 8.

Electrical bulk resistivity test results revealed that the electrical resistivity values follow the same trend with the compressive strength test results for gradually damaged specimens. For instance, the resistivity values at 7, 28, and 90 days ranged in the same order as the compressive strengths for FA-mix and GGBFS-mix, as seen in Fig. 7. Electrical resistivity tests could not be performed on some of the specimens as they lost their integrity after being loaded to failure.

However, for OC-mix and especially SF-mix as seen in Fig. 7, the development of electrical resistivity was slow between 28 and 90 days in contrast to the FA-mix and GGBFS-mix. This situation can be explained by the reaction mechanism that causes the early gain of strength in mixtures containing silica fume and Portland cement or Portland cement alone as a binder and the contribution of FA and GGBFS to the strength relatively later.

When the effect of damage condition on resistivity values is examined, it can be said that there was a slight increase in the values for specimens with 25% damage in general. In other words, the electrical resistivity changed for the level of damage where cracks occurred in the interface area between the aggregate and cement mortar. However, this change was not evident in all mixtures and is slight for the mixtures it was observed. Electrical bulk resistivity values generally did not show a significant change at damage levels between 25% and 75%, where matrix cracks begin to form and develop, while it increases in the damage level between 75% and 100%.

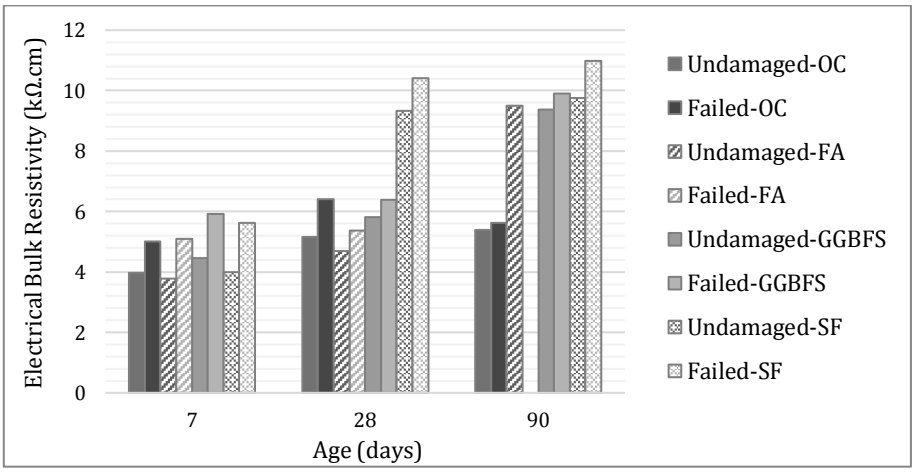

Fig. 7. Electrical bulk resistivity vs. age for each mixture.

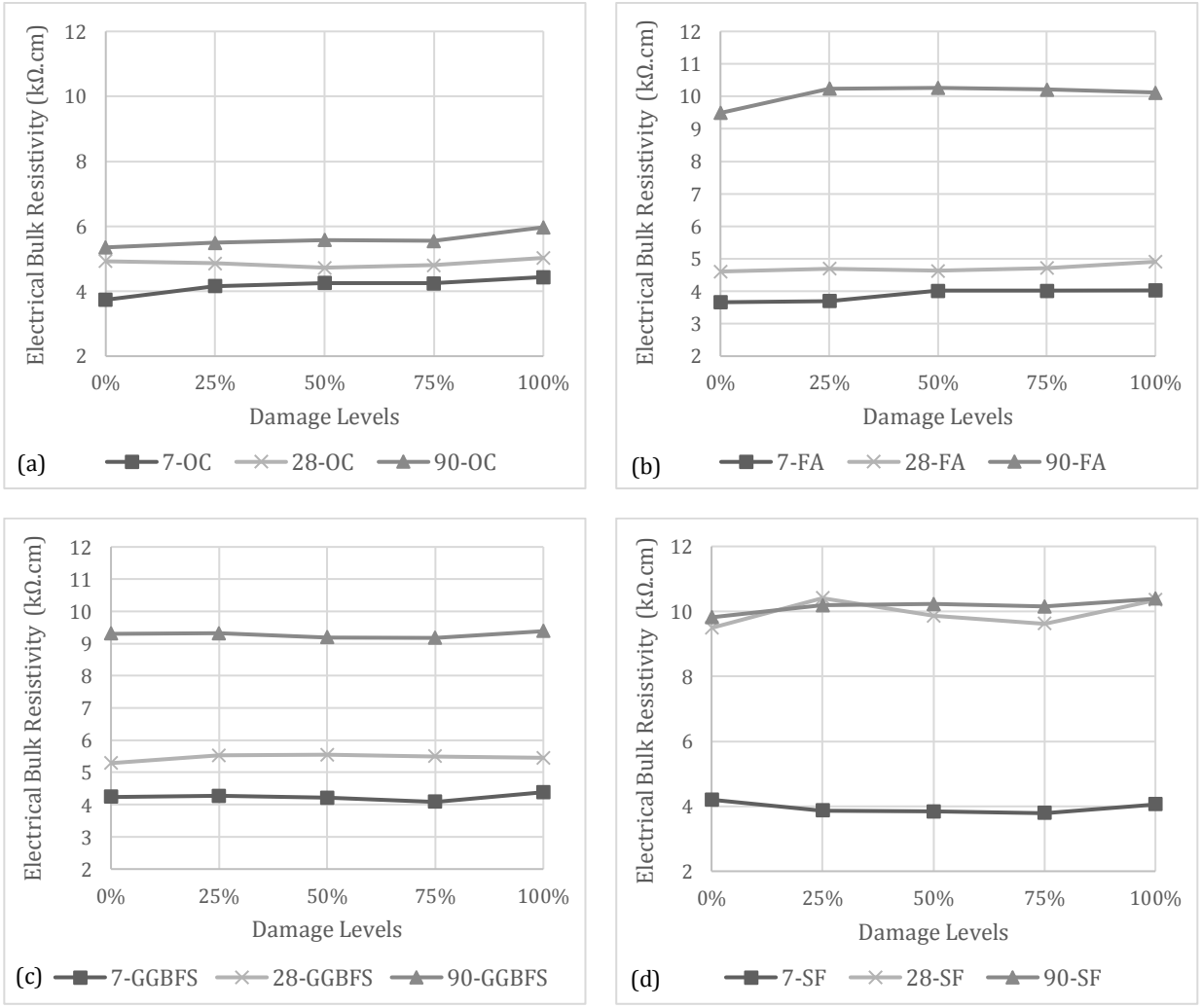

Fig. 8. Electrical bulk resistivity vs. damage levels for each mixture.

3.3. Ultrasonic pulse velocity

In general, ultrasonic pulse velocity values increased with the age of specimens. When observed, the first, second and third points provided the values for the ages of 7, 28 and 90 days respectively in each mixture. To avoid any confusion in the graph, solid filled, blank and pattern filled markers were used to demonstrate 7, 28 and 90 days values. As seen in Fig. 9, the increase in compressive strength depending on the age of the specimen also resulted in an increase in the ultrasonic pulse velocity. The reason for the increase in ultrasonic pulse velocity as the age increases can be regarded as the continuation of the hydration reactions in the concrete and the filling of the

voids in the concrete with C-S-H gels as a result of the hydration reactions. Various studies (Trtnik et al., 2009; Tanyildizi and Coskun, 2008; Lai et al., 2001; Lee and Lee, 2020; Demirboğa et al., 2004; Godinho et al., 2020) have also concluded that the ultrasonic pulse velocity increases when the concrete gains compressive strength.

The ultrasonic pulse velocity values of the control specimens of each mixture for the ages of 7, 28 and 90 days before (undamaged state) and after (failed state) the application of compressive loads up to the failure of the specimens are shown in Fig. 10. Change in the ultrasonic pulse velocity values depending on damage levels is provided in Fig. 11 for each mixture.

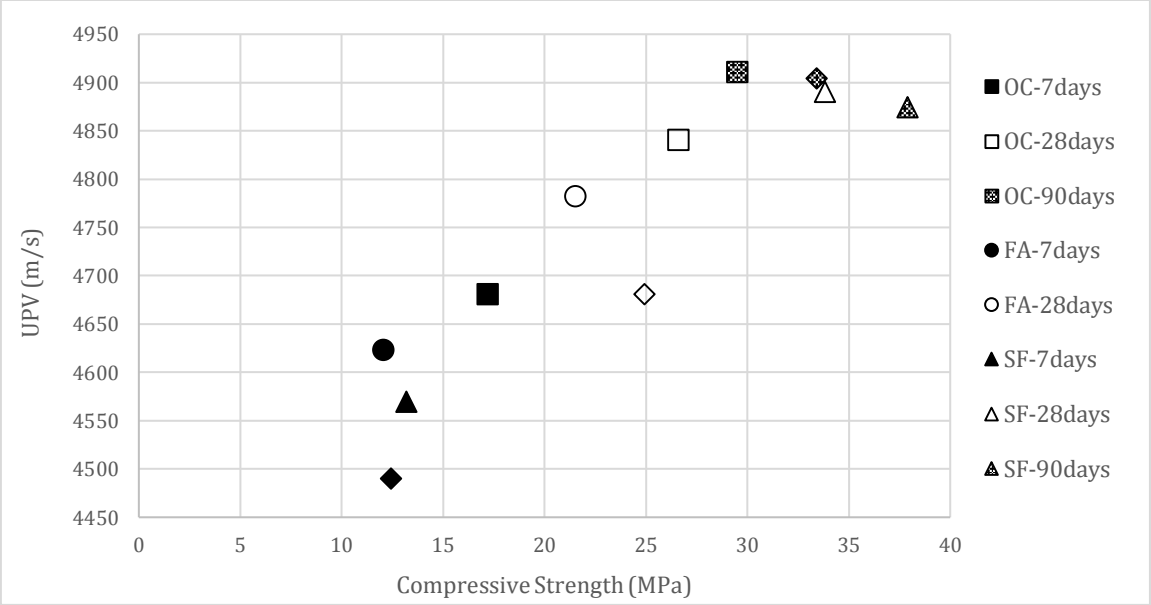

Fig. 9. Ultrasonic pulse velocity vs. compressive strength.

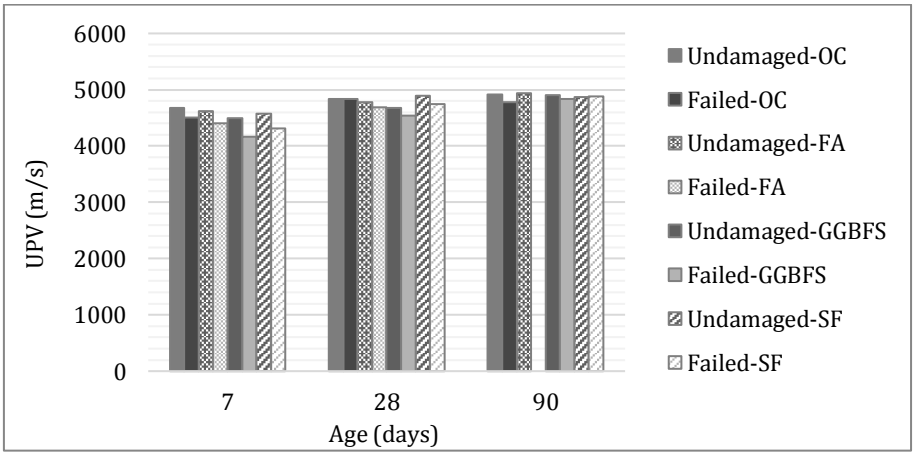

Fig. 10. Ultrasonic pulse velocity vs. age for each mixture.

Ultrasonic pulse velocity results for the OC-mix are given in Fig. 10 and Fig. 11(a). It can be interpreted that the ultrasonic pulse velocity increases as the age of the concrete increases for this mixture. In addition, depending on the extent of concrete damage, decreases in ultrasonic pulse velocity can be mentioned.

In Figs. 10 and 11 ultrasonic pulse velocity developments, depending on age and damage, of FA and SF mixtures can be observed. Since ultrasonic pulse waves cannot pass through the voids inside the concrete, they pass around the voids following a more tortuous path and therefore travel a longer distance. This situation causes a decrease in the ultrasonic pulse velocity of the early age concrete specimen. When the specimens are loaded, the ultrasonic pulse velocity values also decrease. This is because, due to crack formation in the specimen, ultrasonic waves have to travel a longer distance as they go around the cracks.

Ultrasonic pulse velocity results for the GGBFS-mix are given in Figs. 10 and 11(c). It can be interpreted that the ultrasonic pulse velocity increases as the age of the concrete increases for this mixture just as OC-mix. Additionally, depending on the extent of concrete damage, decreases in ultrasonic pulse velocity can be mentioned as well.

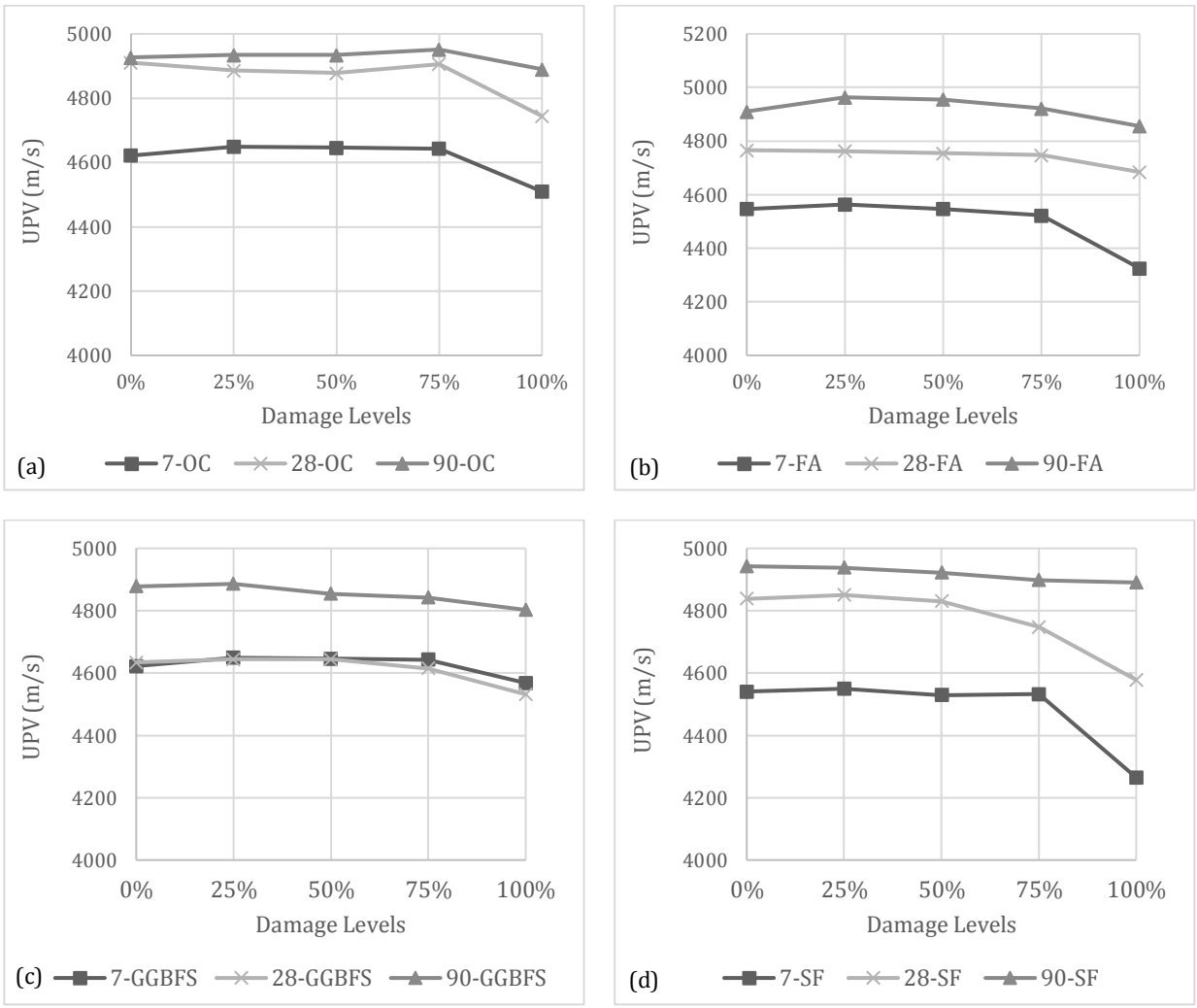

Fig. 11. Ultrasonic pulse velocity vs. damage levels for each mixture.

The ultrasonic pulse velocity showed little variation in gradually damaged concrete specimens regardless of the test age. However, a significant decrease in ultrasonic pulse velocity is observed for all mixtures in the 75%-100% damage level range where matrix cracks develop. From this decrease, it can be concluded that ultrasonic waves pass through the matrix in intact samples and the crack path lengthens only with the increase in the number of cracks in the matrix.

Another inference that can be obtained from the UPV test results is that the velocity decrease for specimens tested at an early age is more significant than in specimens tested at a later age. This may indicate that more matrix cracks occur in low-strength concrete specimens at the same level of damage than high-strength specimens.

3.4. Resonance frequency

Aside from the other NDT tests conducted in this study, resonant frequency measurements could not be conducted at 7 days. For this reason, results were evaluated based on the measurements taken at 28 and 90 days. Dynamic modulus of elasticity values were calculated by using longitudinal resonance frequencies in accordance with ASTM C215 standard. Since the specimen properties are similar, longitudinal resonance frequencies and dynamic modulus of elasticity values can be evaluated in the same way. Dynamic modulus of elasticity was calculated by using Eq. (1).

$$Dynamic\ E = DM(n')^2 \quad (1)$$

where M is the mass of specimen; n' is the fundamental longitudinal frequency (Hz); and D is $5.093 \cdot (L/d^2)$ (m^{-1}) for a cylinder, or $4 \cdot (L/bt)$ (m^{-1}) for a prism.

In the graph below, it should be mentioned that in each mixture, the first and second points provide the values for the ages of 28 and 90 days respectively. To separate the ages, 28 days and 90 days values were shown with blank and pattern filled markers individually. As seen in Fig. 12, the dynamic elasticity modulus that was obtained from the resonance frequency test, as in the ultrasonic pulse velocity test, increased proportionally with the compressive strength of the concrete.

The aged concrete specimens showed a higher dynamic modulus of elasticity as a result of continuous hydration reactions in the concrete and as the existing pores in the concrete are filled with C-S-H gels. Researchers (Lee et al., 1997; Giner et al., 2011) also observed in their study that as the compressive strength of concrete increases, the dynamic modulus of elasticity increases.

The dynamic elastic modulus values of the control specimens of each mixture for the ages of 28 and 90 days before (undamaged state) and after (failed state) the application of compressive loads up to the failure of the specimens are shown in Fig. 13. Variations in the dynamic modulus of elasticity velocity values depending on damage levels are provided in Fig. 14.

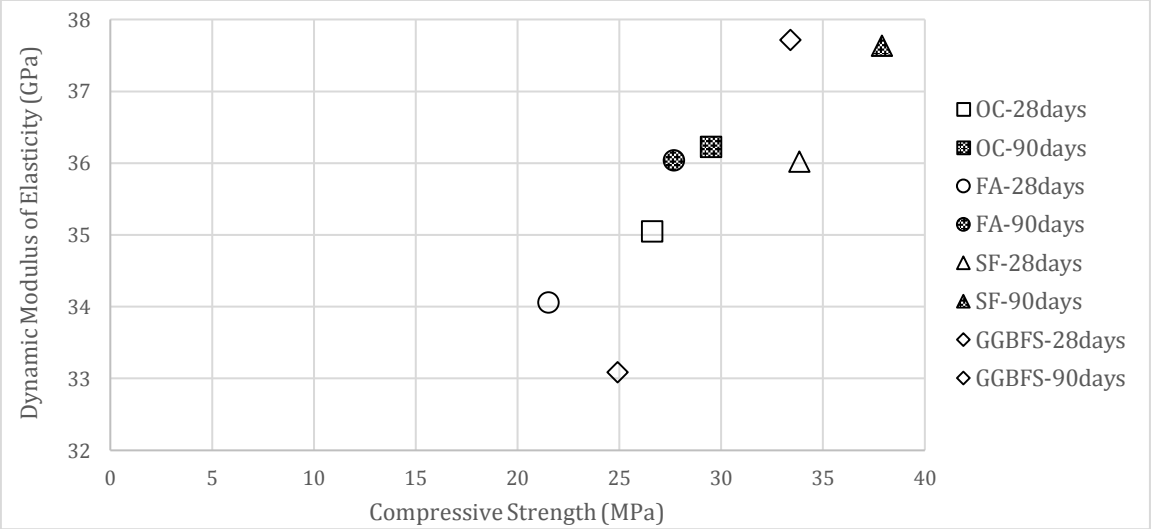

Fig. 12. Dynamic modulus of elasticity vs. compressive strength.

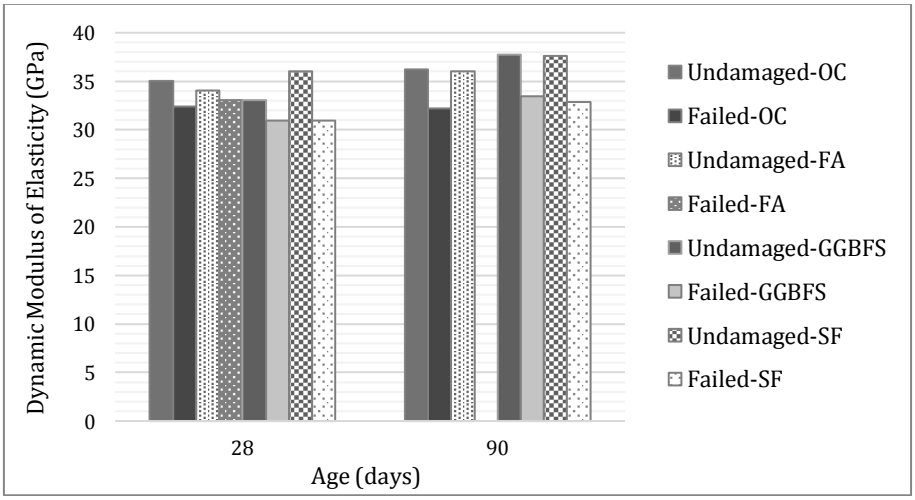

Fig. 13. Dynamic modulus of elasticity vs. age for each mixture.

Considering all the results, the dynamic elasticity modules were obtained from the resonance frequency test results showed a decrease even at the lowest damage level for all concrete mixtures, unlike the electrical resistivity and ultrasonic pulse velocity test results. This decrease is sustained proportional to the damage level, up to the 75% damage level, where interface cracks form and develop and matrix cracks begin to form. This situation is observed regardless of the concrete strength and the binder materials used. In this respect, the resonance frequency test stands out compared to other methods for determining low damage levels. On the other hand, for damage levels between 75% and 100%, the amount of decrease in the dynamic elastic modulus becomes more prominent and observable in all mixtures regardless of concrete strength and binding material type.

When all the results are evaluated together, the most accurate method of measuring concrete damage emerges as the resonance frequency test. For this reason, the diagram given in Fig. 15 was created in order to evaluate the extent of damage depending on the change in the dynamic modulus of elasticity independent of the dynamic elasticity modulus at the undamaged state and therefore the type of binder. As can be seen from the Fig. 15, the dynamic modulus of elasticity obtained from the resonance frequency test immediately decreases even after low damage. With the help of the data presented in the diagram, a third-degree polynomial was drawn to the data in order to obtain the damage amount by using the dynamic elastic modulus values.

When Fig. 15 is inspected it is seen that the vertical axis is between 86 to 100%. This type of presentation is pre-

ferred to make it easier for the reader to understand how the polynomial fits the data. If the vertical axis is chosen between a wider range, it will not be possible to see how the polynomial fits the data. In addition, it is obvious that as the extent of loading increases the data becomes scattered as up to 50% loading a stable system of microcracks form, only after 50-60% cracks start to form in the matrix and after 75 % of interfacial zone becomes unstable and propagation of cracks increase in the matrix and finally spontaneous cracks grow (Mehta and Monteiro, 2006). This is the reason for obtaining a wider data at higher load levels.

Considering the results of all the tests conducted within the scope of this study, electrical resistance and ultrasonic pulse velocity can be used to evaluate the damage of concrete, but the most accurate results can be obtained with the resonance frequency test. The use of resonance frequency test will give more precise results for low damage amount due to higher sensitivity.

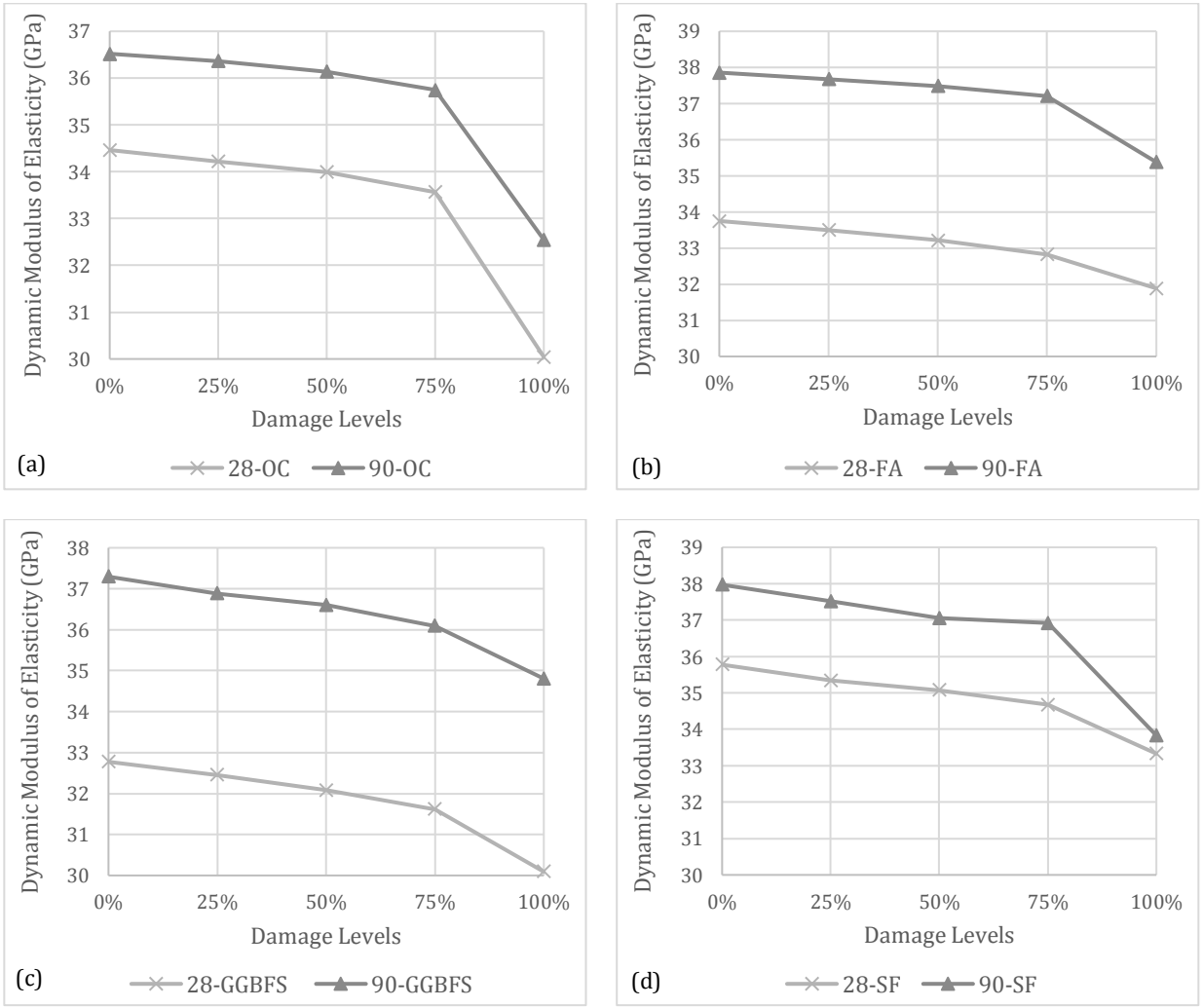

Fig. 14. Dynamic modulus of elasticity vs. damage levels for each mixture.

4. Conclusions

The following conclusions were drawn from the results of the tests conducted throughout the study:

- At the end of the 7th day, the mixture that only contained ordinary Portland cement as a binder showed the highest compressive strength as a result of rapid hydration of cement compared to the other mineral admixtures. However, the gap decreased after 28 days.
- Similar to compressive strength, bulk electrical resistivity results also increased with specimen age as concrete pores are filled with hydration products. Failed specimens had higher bulk electrical resistivities than undamaged specimens as void volume increased, and water saturation of the voids decreased.
- Bulk electrical resistivity results were also changed when specimens were gradually damaged. Between 75% and 100% damage levels, a significant increase was observed in the bulk electrical resistivity.
- Similar to the bulk electrical resistivity, ultrasonic pulse velocity increased with the age of the specimen. As cracks increased in number and volume in damaged concrete, a decrease was observed in the pulse velocity. Similarly, ultrasonic pulse velocity significantly decreased between 75% and 100% damage levels. The extent of this decrease was higher at early ages probably as matrix cracks occur at lower levels of damage in lower strength concrete.

- Contrary to electrical bulk resistivity and ultrasonic pulse velocity, dynamic modulus of elasticity values continually declined up to 75% damage level. This decrease can be explained as cement matrix cracks started to occur and develop. This indicates that resonant frequency potentially predicts the damage level better compared to the other methods. The decrease became more prominent between 75% and 100% damage levels regardless of binding materials and compressive strength of the concrete specimens which makes the resonance frequency test a useful tool to predict the extent of concrete damage.

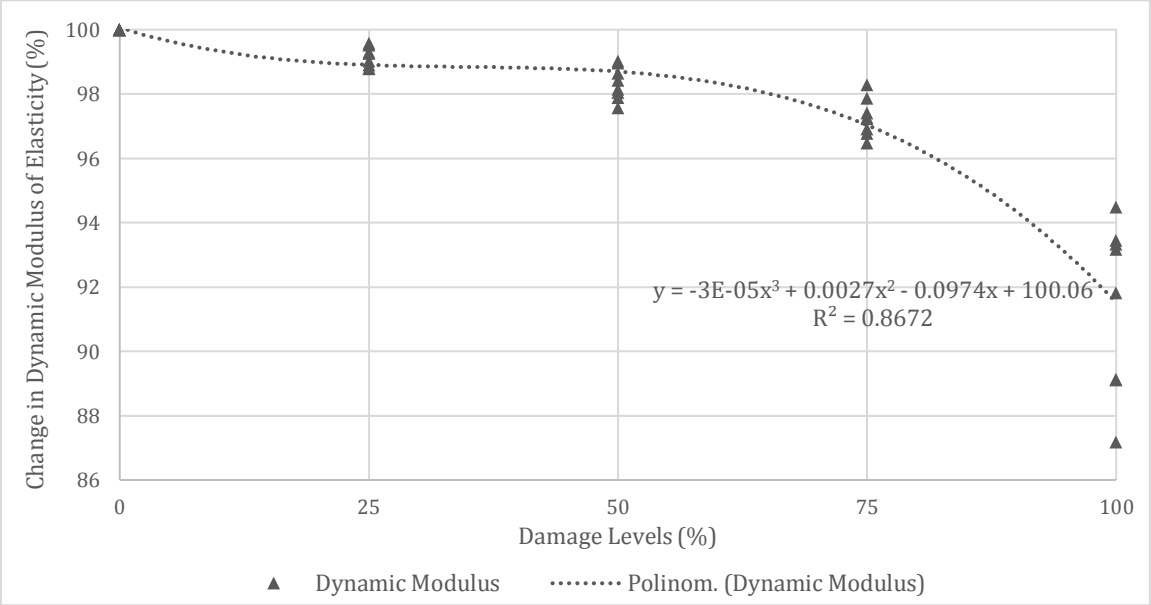

Fig. 15. Change in dynamic modulus vs. damage levels.

Acknowledgements

This study was funded and supported by the Scientific and Technological Research Council of Turkey (TÜBİTAK) under "2020/1 2209-A - Research Project Support Programme for Undergraduate Students" (Application number: 1919B012001306).

References

ACI 211.1-91 (2002). Standard Practice for Selecting Proportions for Normal Heavyweight, and Mass Concrete. American Concrete Institute, Farmington Hills, Michigan, USA.

ACI 228.2R-98 (1998). Nondestructive Test Methods for Evaluation of Concrete in Structures. American Concrete Institute, Farmington Hills, Michigan, USA.

ASTM C39 / C39M-21 (2021). Standard Test Method for Compressive Strength of Cylindrical Concrete Specimens. ASTM International, West Conshohocken, PA, USA.

ASTM C192 / C192M-14 (2014). Standard Practice for Making and Curing Concrete Test Specimens in the Laboratory. ASTM International, West Conshohocken, PA, USA.

ASTM C215-08 (2008). Standard Test Method for Fundamental Transverse, Longitudinal, and Torsional Frequencies of Concrete Specimens. ASTM International, West Conshohocken, PA, USA.

ASTM C597-97 (1997). Standard Test Method for Pulse Velocity through Concrete. ASTM International, West Conshohocken, PA, USA.

Bem DH, Lima DPB, Mederios-Junior RA (2018). Effect of chemical admixtures on concrete´ s electrical resistivity. *International Journal of Building Pathology and Adaptation*, 36 (1), 174-187.

Breysse D (2012). Non-Destructive Assessment of Concrete Structures: Reliability and Limits of Single and Combined Techniques. *Springe*r, Dordrecht, Netherland.

Chun P, Ujike I, Mishima K, Kusumoto M, Okazaki S (2020). Random Forest-based evaluation technique for internal damage in reinforced concrete featuring multiple nondestructive testing results. *Construction and Building Materials*, *253*, 119238.

Demirboğa R, Türkmen İ, Karakoç MB (2004). Relationship between ultrasonic velocity and compressive strength for high-volume mineral-admixtured concrete. *Cement and Concrete Research*, 34, 2329-2336.

Duan P, Shui Z, Chen W, Shen C (2013). Efficiency of mineral admixtures in concrete: Microstructure, compressive strength and stability of hydrate phases. *Applied Clay Science*, 83-84, 115-121.

Duran-Herrera A, De-León-Esquivel J, Bentz DP, Valdez-Tamez P (2019). Self-compacting concretes using fly ash and fine limestone powder: Shrinkage and surface electrical resistivity of equivalent mortars. *Construction and Building Materials*, 199, 50-62.

Ferreira RM, Jalali S (2010). NDT measurements for the prediction of 28-day compressive strength. *NDT&E International*, 43, 55-61.

Gastaldini ALG, Isaia GC, Hoppe TF, Missau F, Saciloto AP (2009). Influence of the use of rice husk ash on the electrical resistivity of concrete: A technical and economic feasibility study. *Construction and Building Materials*, 23, 3411-3419.

Ghoddousi P, Saabadi LA (2017). Study on hydration products by electrical resistivity for self-compacting concrete with silica fume and metakaolin. *Construction and Building Materials*, 154, 219-228.

Giner VT, Ivorra S, Baeza FJ, Zornoza E, Ferrer B (2011). Silica fume admixture effect on the dynamic properties of concrete. *Construction and Building Materials*, 25, 3272-3277.

Godinho JP, De Souza TF, Medeiros MHF, Silva MA (2020). Factors influencing ultrasonic pulse velocity in concrete. *IBRACON Structures and Materials Journal*, 13, 222-247.

Gokce HS, Hatungimana D, Ramyar K (2019). Effect of fly ash and silica fume on hardened properties of foam concrete. *Construction and Building Materials*, 194, 1-11.

Gonen T, Yazicioglu S (2007). The influence of mineral admixtures on the short and long-term performance of concrete. *Building and Environment*, 42, 3080-3085.

Gupta M, Raj R, Sahu AK (2021). Effect of Rice Husk Ash, silica fume & GGBFS on compressive strength of performance based concrete. *Materials Today: Proceedings*.

Hassan KE, Cabrera JG, Maliehe RS (2000). The effect of mineral admixtures on the properties of high-performance concrete. *Cement and Concrete Composites*, 4, 267-271.

Helal J, Sofi M, Mendis P (2015). Non-destructive testing of concrete: A review of methods. *Electronic Journal of Structural Engineering*, 14(1), 97-105.

Hong G, Oh S, Choi S, Chin WJ, Kim YJ, Song C (2021). Correlation between the Compressive Strength and Ultrasonic Pulse Velocity of Cement Mortars Blended with Silica Fume: An Analysis of Microstructure and Hydration Kinetics. *Materials*, 14, 2476.

Kolluru SV, Popovics JS, Shah SP (2000). Determining Elastic Properties of Concrete Using Vibrational Resonance Frequencies of Standard Test Cylinders. *Cement, Concrete, and Aggregates,* CCAGDP, 22 (2), 81-89.

Lai C, Lin Y, Yen T (2001). Behavior and Estimation of Ultrasonic Pulse Velocity in Concrete. *Structural Engineering, Mechanics and Computation*, 2, 1365-1372.

Layssi, G, Ghods, P, Alizadeh, AR, Salehi, M (2015). Electrical Resistivity of Concrete, Concrete International, 37, 5.

Lee KM, Kim DS, Kim JS (1997). Determination of dynamic Young's modulus of concrete at early ages by impact resonance test. *KSCE Journal of Civil Engineering,* 1, 11-18.

Lee T, Lee J (2020). Setting time and compressive strength prediction model of concrete by nondestructive ultrasonic pulse velocity testing at early age. *Construction and Building Materials*, 252.

Lübeck A, Gastaldini ALG, Barin DS, Siqueira HC (2012). Compressive strength and electrical properties of concrete with white Portland cement and blast-furnace slag. *Cement and Concrete Composites*, 34, 392-399.

Medeiros-Junior RA, Lima MG (2016). Electrical resistivity of unsaturated concrete using different types of cement. *Construction and Building Materials*, 107, 11-16.

Mehta PK and Monteiro PJM (2006). Concrete: Microstructure, Properties, and Materials. 3rd Edition. McGraw-Hill, New York.

Mohammed TU, Mahmood AH (2016). Effects of maximum aggregate size on UPV of brick aggregate concrete. *Ultrasonics*, 69, 129-136.

Ozturk M, Karaaslan M, Akgol O, Sevim UK (2020). Mechanical and electromagnetic performance of cement based composites containing different replacement levels of ground granulated blast furnace slag, fly ash, silica fume and rice husk ash. *Cement and Concrete Research*, 136.

Qasrawi HY (2000). Concrete strength by combined nondestructive methods simply and reliably predicted. *Cement and Concrete Research*, 30, 739-746.

Shane JD, Aldea CM, Bouxsein NF, Mason TO, Jenning HM, Shaw SP (1999). Microstructural and pore solution changes induced by rapid chloride permeability test measured by impedance spectroscopy. *Concrete Science and Engineering*, 1, 110-119.

Shi C (2004). Effect of mixing proportions of concrete on its electrical conductivity and the rapid chloride permeability test (ASTM C1202 or ASSHTO T277) results. *Cement and Concrete Research*, 34, 537-545.

Shi H, Xu B, Zhou X (2009). Influence of mineral admixtures on compressive strength, gas permeability and carbonation of high performance concrete. *Construction and Building Materials*, 23, 1980-1985.

Tanyildizi H, Coskun A (2008). Determination of the principal parameter of ultrasonic pulse velocity and compressive strength of lightweight concrete by using variance method. *Russian Journal of Nondestructive Testing*, 44, 639-646.

Trtnik G, Kavčič F, Turk G (2009). Prediction of concrete strength using ultrasonic pulse velocity and artificial neural networks. *Ultrasonics*, 49, 53-60.

Tumidajski PJ (2005). Relationship between resistivity, diffusivity and microstructural descriptors for mortars with silica fume. *Cement and Concrete Research*, 35, 1262-1268.

Valcuende M, Calabuig R, Martínez Ibernó A, Soto J (2020). Influence of Hydrated Lime on the Chloride-Induced Reinforcement Corrosion in Eco-Efficient Concretes Made with High-Volume Fly Ash. *Materials*, 13 (22), 5135.

Yildirim G, Aras GH, Banyhussan QS, Şahmaran M, Lachemi M (2015). Estimating the self-healing capability of cementitious composites through non-destructive electrical-based monitoring. *NDT&E International*, 76, 26-37.